

HOW TO MAKE AN ULTRA-FAINT DWARF SPHEROIDAL GALAXY: TIDAL STIRRING OF DISKY DWARFS WITH SHALLOW DARK MATTER DENSITY PROFILES

EWA L. LOKAS¹, STELIOS KAZANTZIDIS² AND LUCIO MAYER³

Accepted for publication in ApJ Letters on April 19, 2012

ABSTRACT

In recent years the Sloan Digital Sky Survey has unraveled a new population of ultra-faint dwarf galaxies (UFDs) in the vicinity of the Milky Way (MW) whose origin remains a puzzle. Using a suite of collisionless N -body simulations, we investigate the formation of UFDs in the context of the tidal stirring model for the formation of dwarf spheroidal galaxies in the Local Group (LG). Our simulations are designed to reproduce the tidal interactions between MW-sized host galaxies and rotationally supported dwarfs embedded in $10^9 M_\odot$ dark matter (DM) halos. We explore a variety of inner density slopes $\rho \propto r^{-\alpha}$ for the dwarf DM halos, ranging from core-like ($\alpha = 0.2$) to cuspy ($\alpha = 1$), and different dwarf orbital configurations. Our experiments demonstrate that UFDs can be produced via tidal stirring of disky dwarfs on relatively tight orbits, consistent with a redshift of accretion by the host galaxy of $z \sim 1$, and with intermediate values for the halo inner density slopes ($\rho \propto r^{-0.6}$). The inferred slopes are in excellent agreement with those resulting from both the modeling of the rotation curves of dwarf galaxies and recent cosmological simulations of dwarf galaxy formation. Comparing the properties of observed UFDs with those of their simulated counterparts, we find remarkable similarities in terms of basic observational parameters. We conclude that tidal stirring of rotationally supported dwarfs represents a viable mechanism for the formation of UFDs in the LG environment.

Subject headings: galaxies: dwarf — galaxies: fundamental parameters — galaxies: kinematics and dynamics — galaxies: structure — Local Group

1. INTRODUCTION

The Sloan Digital Sky Survey (SDSS) has revealed a new population of dwarf galaxies in the Local Group (LG), known as ultra-faint dwarfs (UFDs) (Willman et al. 2005a,b; Belokurov et al. 2006, 2007, 2008, 2009, 2010; Zucker et al. 2006a,b; Walsh et al. 2007; Irwin et al. 2007). UFDs are typically fainter than $M_V = -8$ mag and extremely metal-poor, and they are located surprisingly close to the Milky Way (MW), mostly within its virial radius. These systems are also believed to be strongly dark matter (DM) dominated, even more than the classic MW dwarf spheroidal galaxies (dSphs) (Simon & Geha 2007; Strigari et al. 2008).

The origin of UFDs is a matter of ongoing debate. Here, we investigate a scenario for their formation based on the tidal stirring model for the origin of classic dSphs in the LG (Mayer et al. 2001). This model relies on the gravitational interaction between initially disky dwarfs and massive host galaxies and its ability to produce classic dSphs has been recently demonstrated (Kazantzidis et al. 2011; Lokas et al. 2011a). In most previous numerical studies, the DM halos of the progenitor dwarfs followed the Navarro, Frenk & White (1997, NFW) density profile and none of the simulations produced an UFD in the end. Recently, however, hydrodynamical simulations of the formation of isolated dwarf galaxies in the

cosmological context have been performed by Governato et al. (2010). These authors modeled inhomogeneous interstellar medium and found that the resulting gas-rich disky dwarfs acquire a significantly shallower inner DM slope relative to the cuspy NFW profiles expected in pure DM simulations, in close agreement with the slopes of observed dwarfs (Oh et al. 2011).

Motivated by the aforementioned developments, we perform for the first time a series of tidal stirring simulations of disky dwarfs embedded in DM halos with different inner density slopes. Our experiments show that the properties of the resulting systems depend very sensitively on the initial inner slope of the DM density profile. More specifically, we demonstrate that tidal stirring of disky dwarfs is capable of producing stellar systems with properties akin to those of UFDs in the LG, provided that the progenitors are placed on relatively tight, eccentric orbits inside MW-sized hosts and are embedded in DM halos with mild central density cusps.

2. THE SIMULATIONS

We employ the method of Widrow et al. (2008) to construct fully self-consistent, equilibrium models of dwarf galaxies consisting of exponential stellar disks embedded in spherical DM halos. The DM density profiles have the form

$$\rho(r) = \frac{\rho_{\text{char}}}{(r/r_s)^\alpha (1 + r/r_s)^{3-\alpha}} \quad (1)$$

with an asymptotic inner $r^{-\alpha}$ and an outer slope r^{-3} (Lokas 2002; Lokas & Mamon 2003). We construct three dwarf galaxies with the same virial mass of $M_{\text{vir}} = 10^9 M_\odot$ and concentration parameter $c = r_{\text{vir}}/r_s = 20$, but different α , which requires slightly different values of

¹ Nicolaus Copernicus Astronomical Center, 00-716 Warsaw, Poland; lokas@camk.edu.pl

² Center for Cosmology and Astro-Particle Physics; and Department of Physics; and Department of Astronomy, The Ohio State University, Columbus, OH 43210, USA; stelios@astronomy.ohio-state.edu

³ Institute for Theoretical Physics, University of Zürich, CH-8057 Zürich, Switzerland; lucio@phys.ethz.ch

the characteristic density ρ_{char} in equation (1). Specifically, we choose $\alpha = 1$ (which corresponds to the NFW profile), and two shallower inner slopes, namely a mild cusp with $\alpha = 0.6$ and a core-like profile with $\alpha = 0.2$. We note that these shallow slopes bracket the range of possible DM slopes inferred from recent cosmological simulations of dwarf galaxy formation at $1 < z < 2$ (Governato et al. 2010).

The DM halos were populated with stellar disks of mass given as a fraction, m_d , of M_{vir} , and we chose $m_d = 0.02$. The adopted disk radial scale length was equal to $R_d = 0.41$ kpc corresponding to a dimensionless spin parameter of $\lambda = 0.04$ (Mo et al. 1998), and the disk thickness was equal to $z_d/R_d = 0.2$, where z_d denotes the vertical disk scale height (see Kazantzidis et al. 2011 regarding the choices for the values of these parameters). For simplicity, we also assumed a constant value for the central radial velocity dispersion $\sigma_{R0} = 10$ km s⁻¹ for all dwarf models. The gross properties of the three dwarfs, including their *total* masses, were very similar. The resulting disks differed only in their planar velocity dispersions and the Toomre Q parameter. Q was equal to 3.8, 3.3 and 2.9 for $\alpha = 1, 0.6$ and 0.2 , respectively, indicating that all disks were stable against bar formation in isolation.

Figure 1 illustrates different properties of our progenitor dwarf models. Although our modeling approach is not unique, our choice of density slopes ensures that the employed DM density profiles (upper panel) have significantly different shapes in the region occupied by the bulk of the stellar component ($\lesssim 2$ kpc), a fact which will be crucial for the interpretation of the results. Moreover, our choices result in dwarf galaxies with different maximum circular velocities, V_{max} (middle panel), with the steeper α corresponding to a larger V_{max} ($V_{\text{max}} = 19.6, 17.8$ and 16.7 km s⁻¹, respectively, for $\alpha = 1, 0.6$ and 0.2). This is important as smaller V_{max} are associated with lower densities in the inner regions and, correspondingly, longer internal dynamical times. Thus, the dwarfs with shallow inner DM slopes are expected to respond more impulsively to the external tidal perturbation and tidal heating will be particularly efficient (Gnedin et al. 1999). Lastly, the binding energy of stars (lower panel) is another key factor that determines their response to tidal shocks. As a result, we expect the dwarfs with shallow cusp slopes to experience much stronger tidal evolution compared to their counterparts with steep cusp slopes.

Each dwarf galaxy model contained $N_h = 10^6$ DM and $N_d = 5 \times 10^5$ disk particles with a gravitational softening of $\epsilon_h = 60$ pc and $\epsilon_d = 20$ pc, respectively. We assumed a single primary galaxy with the present-day structural properties of the MW (Widrow & Dubinski 2005; Kazantzidis et al. 2011). Each of the three dwarfs was placed on five different bound orbits inside the primary galaxy, for a total of 15 numerical experiments. Specifically, we employed orbits R1-R5 of different size and eccentricity from Kazantzidis et al. (2011), with orbital apocenters r_{apo} and pericenters r_{peri} given in kpc in parentheses: R1(125, 25), R2(85, 17), R3(250, 50), R4(125, 12.5), R5(125, 50). In all simulations, the dwarfs were initially placed at the apocenters and the evolution was followed for 10 Gyr. The orientation of the internal angular momentum of all dwarfs with respect to the or-

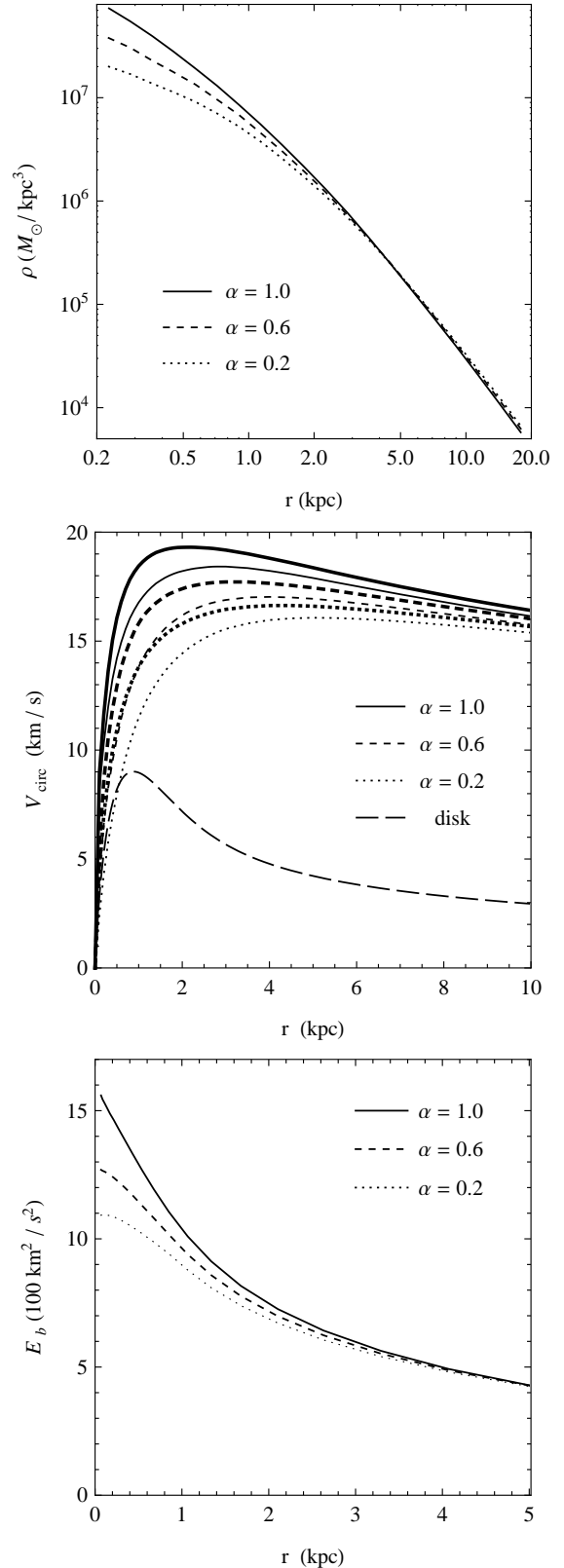


FIG. 1.— The dependence of the initial properties of the adopted dwarf models on the inner slope α . Upper panel: the DM density profiles, middle panel: the disk, halo (thin lines), and total (thick lines) circular velocity profiles, lower panel: the binding energy of the stars per unit mass.

TABLE 1
PARAMETERS OF THE SIMULATED UFDS

Parameter	R2	R4
r_{apo} (kpc)	85	125
r_{peri} (kpc)	17	12.5
T_{orb} (Gyr)	1.3	1.8
N_{apo}	6	6
T_{la} (Gyr)	6.4	9.3
$L_V (10^3 L_\odot)$	6.38	4.84
M_V (mag)	-4.68	-4.38
μ_V (mag arcsec $^{-2}$)	28.3	28.7
$r_{1/2}$ (kpc)	0.166	0.137

bit angular momentum was mildly prograde and equal to $i = 45^\circ$. All numerical experiments were performed with the N -body code PKDGRAV (Stadel 2001).

3. THE FORMATION AND PROPERTIES OF SIMULATED UFDS

The tidal evolution of our dwarfs follows the general picture established in earlier works (see Mayer et al. 2001, 2007; Klimentowski et al. 2007, 2009; Kazantzidis et al. 2011; Lokas et al. 2011b). In particular, all dwarf galaxies undergo mass loss, their morphology changes from a disk to a triaxial and then to a more spherical shape, and the stellar rotation is transformed into random motions. The degree of these changes is sensitive to the orbital configuration, namely it is proportional to the total tidal force experienced by the dwarfs (see Lokas et al. 2011c) but also depends on the structural properties of the progenitors (Kazantzidis et al. 2011; Lokas et al. 2011a,b).

Here we attempt to investigate the effect of the inner cusp of the DM halo. We note that the dependence of the overall morphological transformation of the dwarfs on the inner density slope will be discussed in a future work; here we only mention that dwarfs with shallower cusps are more susceptible to changes, they lose mass more effectively and are thus more easily destroyed with obvious implications for the missing satellites problem. In particular, dwarfs with the standard NFW cusp of $\alpha = 1.0$ survive until the end of the simulation for all orbits, while dwarfs with the shallowest inner profile with $\alpha = 0.2$ are dissolved completely for the tighter orbits R1, R2 and R4 after 4, 3 and 2 pericenter passages, respectively. The destruction of these dwarfs occurs rather early in the evolution, when the dwarfs are still quite massive, via elongation of the bar formed at an earlier stage. On the other hand, the intermediate cusp of $\alpha = 0.6$ leads to a longer survival, but the dwarfs become much smaller in size.

In what follows, we focus on the evolution of dwarfs with $\alpha = 0.6$ on orbits R2 and R4 which leads to the formation of dSph galaxies with properties akin to those of present-day UFDS in the vicinity of the MW. The two orbits are plotted in the upper panel of Figure 2 up to the sixth apocenter, the last one at which the dwarfs are still discernible. The initial apo- and pericenter distances of these orbits, r_{apo} and r_{peri} , their orbital times T_{orb} , number of apocenters after which the dwarfs are identified, N_{apo} , and times when these last apocenters took place (from the start of the simulation), T_{la} , are listed in the first five rows of Table 1.

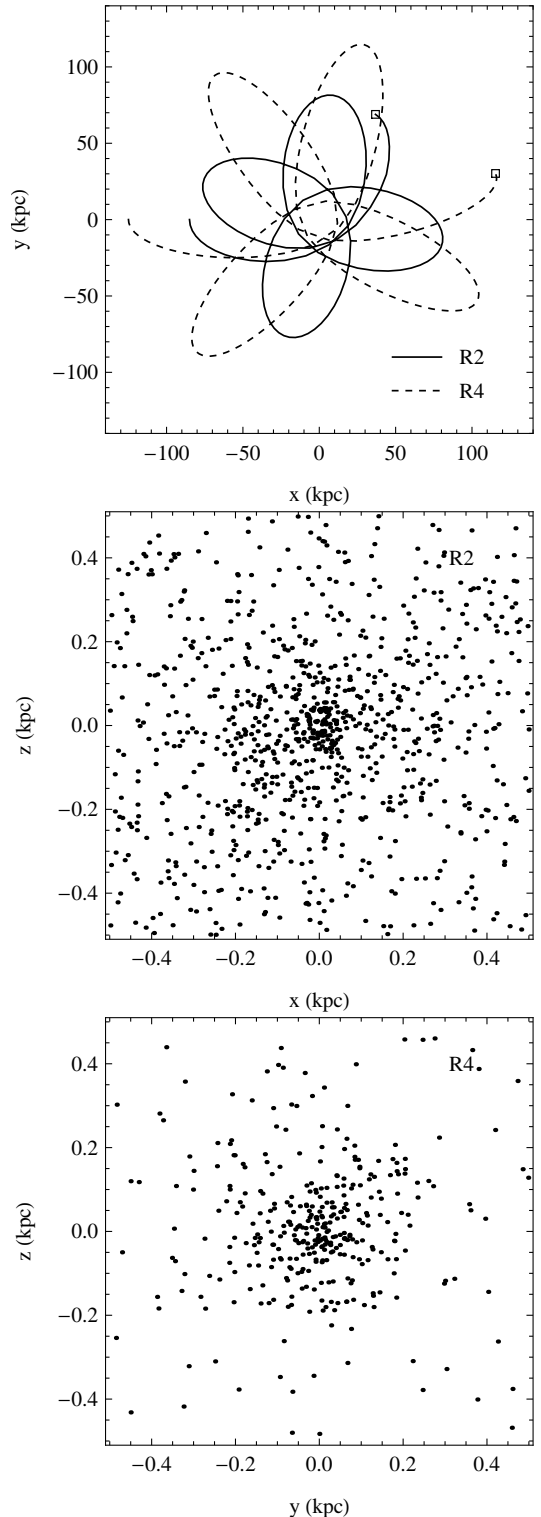


FIG. 2.— Upper panel: The orbits of dwarfs in simulations R2 and R4. The orbits run anti-clockwise from the initial apocenter on the left up to the sixth apocenter marked with an open square. Middle and lower panel: The stars in our simulated UFD galaxies identified at the sixth apocenter of runs R2 and R4 with $\alpha = 0.6$. The images show 907 and 356 stars for R2 and R4 respectively, contained in a box of 1 kpc on a side and centered on the dwarf. The positions of the stars were projected along the y (for R2) and x (for R4) axis of the simulation box.

The stellar components of the dwarfs at the sixth apocenter are shown in the two lower panels of Figure 2. The stars of the dwarfs and their immediate surroundings were selected from a box of size 1 kpc and their positions projected along one direction. The dwarfs thus appear as they would be seen by a distant observer looking at them along one axis of the simulation box if the observer was able to subtract the contamination from the MW and the more distant tidal debris from the dwarf itself. The very low numbers of the stars (907 and 356 for R2 and R4) mean that the dwarfs would only appear as very small overdensities against the background (see below).

In Figure 3 we present stellar number density profiles in the dwarfs formed in runs R2 and R4. The density was measured by counting stars in logarithmically spaced bins of radius starting from 3 softening scales of stellar particles. In each panel the curves from top to bottom correspond to measurements performed at subsequent apocenters, from the second to the sixth. The evolution of the density profiles, and more specifically the decrease of the normalization, reflects the stellar mass loss occurring as a result of the interaction with the host galaxy. In addition, this Figure demonstrates that tidal shocks do not serve to modify the central density cusp of the stellar distribution, in agreement with the study of Kazantzidis et al. (2004) where pure DM satellites were evolved inside a static host potential. Lastly, each density profile shows a characteristic transition from the bound stellar component to the tidal tails, marked by an abrupt change in the outer slope of the profile, from the steeper to the shallower. This change occurs at smaller radii for subsequent apocenters signifying the decreasing size of the dwarf.

In order to quantify this evolution we fitted each profile with the Plummer formula estimating the half-light radius $r_{1/2}$ and normalization. The fits were done only to data points (weighted by density) within the range of radii unaffected by tidal tails. The fitted normalization, which is the total number of stars, multiplied by the stellar mass and the stellar mass-to-light ratio, gives the total luminosity of the dwarf at each apocenter L_V or equivalently its visual magnitude M_V . For the stellar mass-to-light ratio we adopt a constant value $M/L_V = 2.5M_\odot/L_\odot$ as predicted for the present time for a simple low-metallicity stellar population in the standard model described by Bruzual & Charlot (2003). Thus at all stages, the luminosities of the simulated dwarfs can be directly compared to the properties of the real MW UFDs.

We also measured the central surface brightness μ_V of the dwarfs at each stage by first selecting the stars within $5r_{1/2}$ from the center and then counting stars contained within a cylinder of radius $0.2r_{1/2}$ along the three axes of the simulation box. The final value follows from the average number of stars measured in the three directions. The values of all the observational parameters of the two dwarfs at the sixth apocenter are listed in the last four rows of Table 1.

We summarize the evolution of these properties by plotting in Figure 4 the evolutionary tracks of the dwarfs in simulations R2 and R4 in the M_V - μ_V and M_V - $r_{1/2}$ planes. We include as crosses analogous properties for 10 other of our simulated dwarfs which survive until the

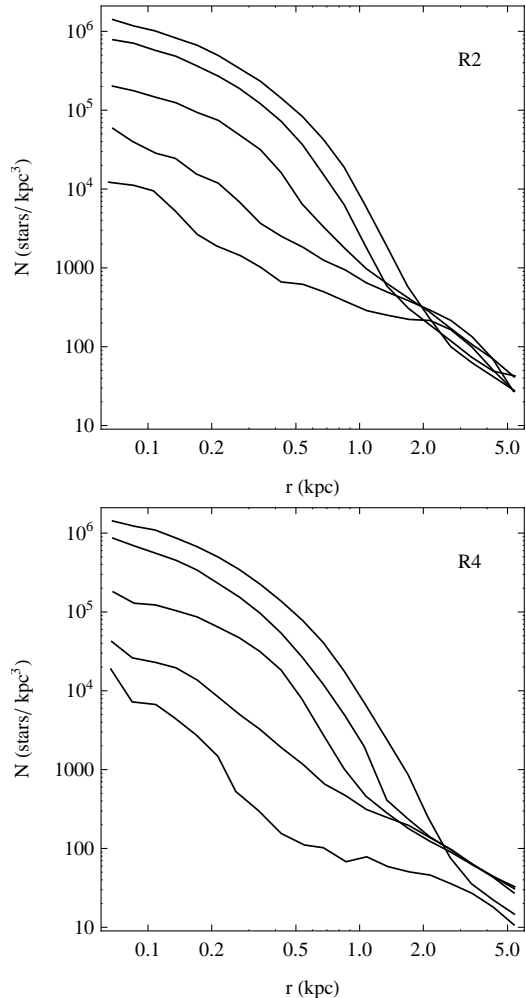


FIG. 3.— Stellar number density profiles of the dwarf galaxies measured at subsequent apocenters for simulation R2 (upper panel) and R4 (lower panel) with $\alpha = 0.6$. The solid lines in each panel show decreasing stellar densities from the second to the sixth apocenter (from the top to the bottom curve).

end much brighter and are thus more akin to classic dSph galaxies of the LG (see Figure 20 in Lokas et al. 2011a). We also show with circles the parameters of the real MW UFDs, as determined by Martin et al. (2008). The brightest dwarfs, with $M_V < -8$ mag, are the Canes Venatici I dwarf ($M_V = -8.6$) and Draco ($M_V = -8.75$). Draco is usually considered as one of the classic dSphs, but its luminosity indicates that it is rather a border-line case between the brighter population of classic dwarfs and the UFDs.

The comparison of the evolutionary tracks of the simulated dwarfs to the real data proves that the tidal stirring indeed brings the initially massive subhalos possessing mild inner DM cusps and populated with a standard stellar disk to regions of parameter space occupied by UFDs found around the MW. The end products of runs R2 and R4, although tracing different orbits around the host, are similar to each other and particularly close in their observational properties to the UFD Ursa Major II with $M_V = -4.2$ mag, $\mu_V = 27.9$ mag arcsec $^{-2}$, and $r_{1/2} = 0.140$ kpc (Martin et al. 2008). Although our values of the central surface brightness are a little below

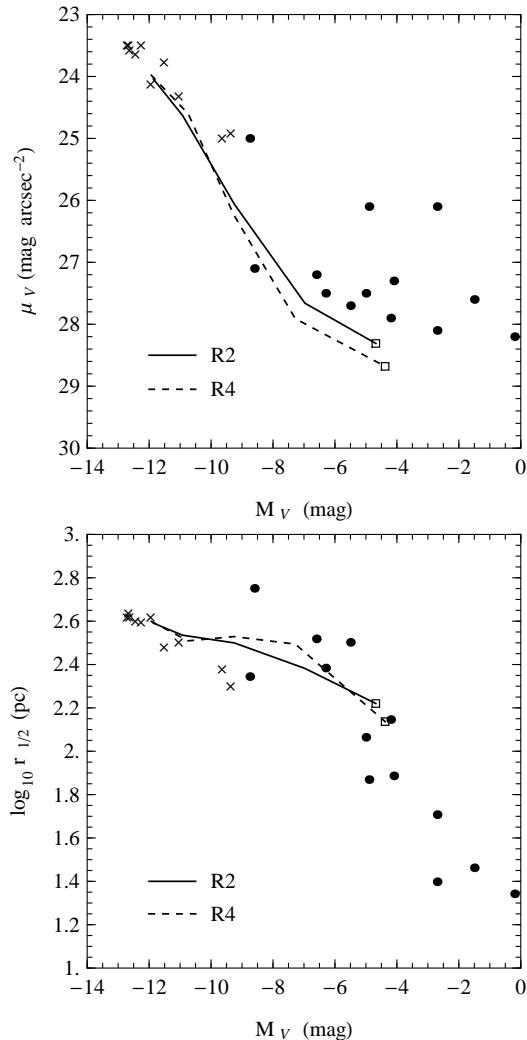


FIG. 4.— Evolutionary tracks of the simulated dwarfs in runs R2 and R4 with $\alpha = 0.6$ in the M_V - μ_V (upper panel) and M_V - $r_{1/2}$ (lower panel) planes. The solid and dashed lines (for R2 and R4, respectively) join the values of the parameters measured at subsequent apocenters from the second to the sixth. Open squares mark the final values measured at the sixth apocenter. Crosses indicate observational parameters at the last apocenter for 10 dwarfs (on orbits R1-R5 and with different α) which did not end up as UFDs, but survived for 10 Gyr. Circles show values of the analogous parameters for the real UFDs of the MW.

the observed range, we note that the real dwarfs may be contaminated by MW stars and therefore have their brightnesses overestimated. Still, our simulated dwarfs should be discernible above the background level due to the tidally stripped stars which we estimate to be of the order of 31.2 and 32.4 mag arcsec $^{-2}$ at $5r_{1/2}$ for R2 and R4 respectively.

4. DISCUSSION

Using collisionless N -body simulations, we have demonstrated that the tidal stirring of $\sim 10^9 M_\odot$ disk dwarfs for a period of ~ 8 Gyr can lead to the formation of stellar systems with properties akin to those of UFDs around the MW. Specifically, our experiments have shown that UFDs are produced when the progenitor disk dwarfs are placed on relatively tight ($r_{\text{peri}} \lesssim$

20 kpc), eccentric ($r_{\text{apo}}/r_{\text{peri}} \gtrsim 5$) orbits inside a MW-sized host and are embedded in DM halos with a mild central density cusp ($\rho \propto r^{-0.6}$).

Such slopes agree with those inferred from both the modeling of rotation curves of dwarf galaxies (Oh et al. 2011) and recent cosmological simulations of dwarf galaxy formation (Governato et al. 2010). In the latter work, cusp flattening occurs as a result of potential fluctuations induced by rapid removal of baryons via supernovae winds, a mechanism that depends both on the stellar and halo mass. Because our models lack gas, dissipation and star formation, a direct comparison with Governato et al. is difficult. However, we note that the baryonic and halo masses of the Governato et al. dwarfs at $z > 1$ are similar to those adopted in the present study (within a factor of a few). This together with the fact that satellite accretion is a generic feature of hierarchical models of structure formation suggests that the model described in this study should be applicable to at least some of the UFDs in the LG.

According to the impulsive approximation (which should be valid in our simulations for the purposes of dimensional analysis), the energy injected at each pericentric passage is given by $\Delta E \propto M_{\text{host}}^2 M R^2 V_{\text{rel}}^{-2}$, where M_{host} is the mass of the host, R is a characteristic radius of the dwarf (related to the distance from the center of the dwarf where V_{max} occurs, r_{max}), M is a characteristic mass related to the mass of the dwarf within r_{max} , and V_{rel} is the relative velocity between the two galaxies at the pericenter of the orbit (Binney & Tremaine 2008). Given that M_{host} is the same and V_{rel} is fairly similar for a given orbit, $\Delta E \propto M R^2$.

By virtue of the virial theorem, the energy content of the dwarf should scale as $E \propto M^2/R$. Hence, the fractional increase in energy caused by the tidal shocks is given by $\Delta E/E \propto R^3/M$. Increasing cusp slopes correspond to smaller R^3/M , and thus to smaller $\Delta E/E$. This explains why for $\alpha = 1$ the dwarfs experience a moderate amount of mass loss and survive, while they are completely disrupted in the $\alpha = 0.2$ case which is associated with the largest $\Delta E/E$. On the other hand, the magnitude of tidal shocks when $\alpha = 0.6$ lies in between the two aforementioned cases, explaining naturally the evolution of these dwarfs towards UFDs.

Our simulations produce UFDs with $M_V > -5$ mag, $\mu_V = 28$ -29 mag arcsec $^{-2}$, and $r_{1/2} = 0.1$ -0.2 kpc. These observational properties are very similar to those of the observed population of MW UFDs. This is valid for dwarfs evolved on fairly tight orbits, consistent with distances interior to 100 kpc of 6 out of the 11 UFDs discussed in e.g. Kalirai et al. (2010), whereas on less tight orbits remnants resembling classic dSphs still result even for these shallow profiles.

One may wonder if the similarities extend to other properties of UFDs, such as their inferred high DM content. The global M/L values at a scale of 1 kpc in both simulated UFDs are of the order of 10-20 M_\odot/L_\odot . Admittedly, these M/L ratios are lower than the values normally quoted for UFDs (Kalirai et al. 2010). Note, however, that the progenitors could have started out with most of the cold baryons in the gaseous phase. Then ram pressure stripping aided by heating from the ionizing background would remove most of them before

they turned into stars, possibly leaving behind an object with the same halo mass as our UFD-like remnants but lower stellar mass. These processes, in association with tidal stirring, have already been shown to explain the most DM-dominated among classic dSphs, such as Draco (Mayer et al. 2007). In addition, kinematic samples of UFDs are likely contaminated by tidally stripped and MW stars, which could artificially enhance the measured M/L .

Other models for the origin of UFDs, such as the reionization fossil scenario (Ricotti & Gnedin 2005; Gnedin et al. 2008), would not produce a correlation between UFDs and orbital distance, but could explain the existence of UFDs at large distances from the primaries, like Leo T (Irwin et al. 2007). In such models the halo mass of

the progenitor would be lower ($< 10^8 M_\odot$). The different progenitor halo masses should result in different overall numbers of the UFDs at $z = 0$, both because halo mass affects survival rate and the number of subhalos at different mass scales are different. The statistics of the population of UFDs combined with orbital information could thus be a way to constrain formation models.

This research was partially supported by the Polish National Science Centre under grant NN203580940. S.K. is supported by the Center for Cosmology and Astro-Particle Physics at The Ohio State University. The numerical simulations were performed at the Ohio Supercomputer Center (<http://www.osc.edu>).

REFERENCES

- Belokurov, V., Zucker, D. B., Evans, N. W., et al. 2006, *ApJ*, 647, L111
- Belokurov, V., Zucker, D. B., Evans, N. W., et al. 2007, *ApJ*, 654, 897
- Belokurov, V., Walker, M. G., Evans, N. W., et al. 2008, *ApJ*, 686, L83
- Belokurov, V., Walker, M. G., Evans, N. W., et al. 2009, *MNRAS*, 397, 1748
- Belokurov, V., Walker, M. G., Evans, N. W., et al. 2010, *ApJ*, 712, L103
- Binney, J., & Tremaine, S. 2008, *Galactic Dynamics* (Princeton: Princeton Univ. Press)
- Bruzual, G., & Charlot, S. 2003, *MNRAS*, 344, 1000
- Gnedin, O. Y., Hernquist, L., & Ostriker, J. P. 1999, *ApJ*, 514, 109
- Gnedin, N. Y., Kravtsov, A. V. & Chen, H.-W., 2008, *ApJ*, 672, 765
- Governato, F., Brook, C., Mayer, L., et al. 2010, *Nature*, 463, 203
- Irwin, M. J., Belokurov, V., Evans, N. W., et al. 2007, *ApJ*, 656, L13
- Kalirai, J., Beaton, R. L., Geha, M. C., et al. 2010, 711, 671
- Kazantzidis, S., Mayer, L., Mastrogiuseppe, C., Diemand, J., Stadel, J., & Moore, B. 2004, *ApJ*, 608, 663
- Kazantzidis, S., Lokas, E. L., Callegari, S., Mayer, L., & Moustakas, L. A. 2011, *ApJ*, 726, 98
- Klimontowski, J., Lokas, E. L., Kazantzidis, S., Prada, F., Mayer, L., & Mamon, G. A. 2007, *MNRAS*, 378, 353
- Klimontowski, J., Lokas, E. L., Kazantzidis, S., Mayer, L., & Mamon, G. A. 2009, *MNRAS*, 397, 2015
- Lokas, E. L. 2002, *MNRAS*, 333, 697
- Lokas, E. L., & Mamon, G. A. 2003, *MNRAS*, 343, 401
- Lokas, E. L., Kazantzidis, S., & Mayer, L. 2011a, *ApJ*, 739, 46
- Lokas, E. L., Majewski, S. R., Kazantzidis, S., et al. 2011b, *ApJ*, in press, arXiv:1112.5336
- Lokas, E. L., Kazantzidis, S., Mayer, L., & Callegari, S. 2011c, in *Astrophysics and Space Science Proceedings, Environment and the Formation of Galaxies: 30 years later*, ed. I. Ferreras & A. Pasquali (Berlin Heidelberg: Springer-Verlag), 229
- Martin, N. F., de Jong, J. T. A., & Rix, H.-W. 2008, *ApJ*, 684, 1075
- Mayer, L., Governato F., Colpi, M., et al. 2001, *ApJ*, 559, 754
- Mayer, L., Kazantzidis, S., Mastrogiuseppe, C., & Wadsley, J. 2007, *Nature*, 445, 738
- Mo, H. J., Mao, S., & White, S. D. M. 1998, *MNRAS*, 295, 319
- Navarro, J. F., Frenk, C. S., & White, S. D. M. 1997, *ApJ*, 490, 493 (NFW)
- Oh, S.-H., Brook, C., Governato, F., et al. 2011, *AJ*, 142, 24
- Ricotti, M., & Gnedin, N. Y. 2005, *ApJ*, 629, 259
- Simon, J. D., & Geha, M. 2007, *ApJ*, 670, 313
- Stadel, J. G. 2001, PhD thesis, Univ. of Washington
- Strigari, L. E., Bullock, J. S., Kaplinghat, M., et al. 2008, *Nature*, 454, 1096
- Walsh, S. M., Jerjen, H., & Willman, B. 2007, *ApJ*, 662, L83
- Widrow, L. M., & Dubinski, J. 2005, *ApJ*, 631, 838
- Widrow, L. M., Pym, B., & Dubinski, J. 2008, *ApJ*, 679, 1239
- Willman, B., Blanton, M. R., West, A. A., et al. 2005a, *AJ*, 129, 2692
- Willman, B., Dalcanton, J. J., Martinez-Delgado, D., et al. 2005b, *ApJ*, 626, L85
- Zucker, D. B., Belokurov, V., Evans, N. W., et al. 2006a, *ApJ*, 643, L103
- Zucker, D. B., Belokurov, V., Evans, N. W., et al. 2006b, *ApJ*, 650, L41